HNUE JOURNAL OF SCIENCE
Natural Sciences 2025, Volume 70, Issue 2, pp. 70-77
This paper is available online at http://hnuejs.edu.vn/ns
DOI: 10.18173/2354-1059.2025-0022

SYNTHESIS AND OPTICAL PROPERTIES OF NITROGEN-DOPED CARBON QUANTUM DOTS

Le Thi Kim Dung[1], Nguyen Vinh Phu[1], Nguyen Nhu Y[2] and Nguyen Minh Hoa[1,*]
[1]*Faculty of Fundamental Sciences, Hue University of Medicine and Pharmacy, Hue University, Hue city, Vietnam*
[2]*School of Engineering and Technology, Hue University, Hue city, Vietnam*
[*]Corresponding author: Nguyen Minh Hoa, e-mail: nguyenminhoa@hueuni.edu.vn

Received January 10, 2025. Revised May 10, 2025. Accepted June 30, 2025.

Abstract. Nitrogen-doped carbon quantum dots (N-CQDs) were successfully synthesized using a hydrothermal method at 150 °C for 3 hours, with glucose and urea serving as the carbon and nitrogen precursors, respectively. The resulting N-CQDs, which had an average particle size of 3.60 ± 0.57 nm, exhibited blue fluorescence with an emission peak approximated 485.5 nm when excited at 370 nm. The photoluminescence intensity of the N-CQDs was pH-dependent, reaching its maximum at pH 5.0. Fourier transform infrared spectroscopy analysis revealed that the surface of the N-CQDs contained functional groups with carbon, nitrogen, and oxygen bonds, which contributed to their excellent water solubility and strong blue photoluminescence (quantum yield of 23%). These properties indicate that N-CQDs have high potential for applications in bioimaging and biosensing.

Keywords: quantum dots, nitrogen-doped carbon, optical properties, N-CQDs, hydrothermal synthesis.

1. Introduction

Semiconductor quantum dots (QDs) are luminescent nanomaterials with unique properties that have been studied for over 25 years. Their optical and electronic properties can be tuned through control of their size, shape, and chemical composition [1]. QDs belonging to the II-VI and III-V groups have demonstrated significant advantages in various applications, including bioimaging [2], solar cells [3], light-emitting devices [4], luminescent materials, and field-effect transistors [2].

However, many materials based on elements from these groups contain heavy metals, and their toxicity poses significant challenges for biological and environmental applications [5], [6]. This has made the development of alternative QDs with good optoelectronic properties, based on less toxic materials. This need has spurred the development of new, heavy-metal-free materials, such as group IV materials (Si, Ge, C) and some ternary

compounds in the I-III-VI group [7]. Recently, carbon-based nanomaterials have emerged as a promising, non-toxic, cost-effective, and biocompatible alternative, attracting significant attention [8], [9]. The various forms of carbon nanomaterials, such as graphene quantum dots, carbon quantum dots (CQDs), and carbon nanodots, exhibit unique optical properties related to their respective structural characteristics, which are primarily determined experimentally [10]. In particular, CQDs, with their low toxicity and promising optical properties, are being explored for applications in sensing, bioimaging, drug delivery, photodynamic therapy, photocatalysis, luminescent materials, light-emitting devices, and optoelectronic devices [11], [12]. Further modifications of CQDs, such as nitrogen doping, are of great interest for enhancing their properties.

Currently, CQD synthesis faces challenges, including high costs, complex procedures, and the use of toxic chemical precursors [13]. Biomass-derived precursors offer a promising "green" alternative [14], potentially reducing costs and environmental impact. However, these methods often struggle with poor control over particle size, quality, and sample uniformity, frequently resulting in CQDs with poor optical properties and low photoluminescence quantum yield (PLQY) [15]. Doping with elements like N, P, and S is a common approach to improve these properties [16], yet optimal methods and the underlying mechanisms remain unclear. Conventional methods like microwave synthesis suffer from rapid, uncontrollable doping processes and high energy consumption [17].

In contrast, the hydrothermal method offers several advantages: ease of implementation, environmental friendliness, low cost, and the ability to produce photostable CQDs. This approach allows for better control over synthesis parameters, addressing the limitations of previous methods and providing a suitable platform for investigating nitrogen doping and its impact on the optical properties of CQDs.

In this study, we used a hydrothermal method to synthesize nitrogen-doped carbon quantum dots (N-CQDs) from glucose and urea via hydrothermal treatment, addressing the challenges of using toxic precursors. Our focus was to investigate the synthesis parameters, optical properties, and their potential for applications such as bioimaging and optical sensing. The incorporation of nitrogen into the carbon structure of CQDs has been shown to enhance their fluorescence properties. Our results also suggest that these N-CQDs have potential for applications such as bioimaging and optical sensing.

2. Content

2.1. Experimental methods

2.1.1. Chemicals

Chemicals, glucose, and urea (Sigma-Aldrich) were used as received, and double-distilled water was used throughout this study.

2.1.2. Synthesis of nitrogen-doped carbon quantum dots (N-CQDs)

The N-CQDs were synthesized using a hydrothermal method. A homogeneous mixture was prepared by dissolving 5 mmol of glucose and 10 mmol of urea in 40 mL of deionized water. This mixture was then transferred into a Teflon-lined hydrothermal reactor, which was sealed and placed in an oven at 150°C for 3 hours. Afterward, the reactor was allowed to cool naturally to room temperature. The resulting solution was

filtered through a 0.22 µm filter and then centrifuged at 10,000 rpm to remove unreacted precursors and byproducts. The purified solution was then dried in a vacuum oven overnight at 80 °C to obtain the N-CQD powder.

2.1.3. Characterization

UV-Vis spectra of the samples were measured using a Shimadzu UV-1800 spectrophotometer in the wavelength range of 300 to 800 nm. Photoluminescence (PL) spectra of the N-CQDs were measured using a Horiba FL3-22 fluorescence spectrometer. The size of the samples was determined from transmission electron microscopy (TEM) images using a JEOL 2100 (200 kV, Japan) microscope. Energy-dispersive X-ray spectroscopy (EDS) analysis of the samples was conducted using a Hitachi SU-8010 SEM with a scan speed of 10 s. Fourier transform infrared (FTIR) spectra were obtained using a Jasco International FT/IR-6700 spectrometer with a scan range between 400 and 4000 cm^{-1}. The photoluminescence quantum yield (PLQY) of the samples was measured directly using an Edinburgh Instruments FLS1000 Spectrometer.

2.1.4. Investigation of pH effects

To investigate the impact of pH on the N-CQD's optical properties, the pH of a 1mg/mL N-CQD solution was adjusted using solutions of diluted NaOH (1.0 M) and HCl (1.0 M), to obtain solutions with pH ranging from 2 to 9. A Hach sensION+ PH3 pH meter was used to determine the corresponding pH values. All measurements were taken at room temperature.

2.2. Results and discussion

2.2.1. Morphological and structural characterization of N-CQDs

The TEM images (Figure 1(a)) reveal that the N-CQDs exhibit a predominantly spherical morphology with some degree of aggregation, displaying a particle size distribution ranging from approximately 2 to 6 nm. The particle size distribution (inset of Figure 1(a)), fitted to a Gaussian distribution, exhibits an average particle size of 3.60 ± 0.57 nm. Scanning electron microscopy coupled with energy-dispersive X-ray spectroscopy analysis (Figure 1(b)) shows that the material is composed of approximately 70.91 wt% C, 19.13 wt% O, and 9.96 wt% N (Table in the inset of Fig. 1b), confirming successful synthesis of the N-CQDs with the desired nitrogen doping. This elemental composition, with atomic percentages of 78.54 % C, 15.94 % O, and 5.19 % N, supports the successful incorporation of nitrogen into the carbon quantum dot structure.

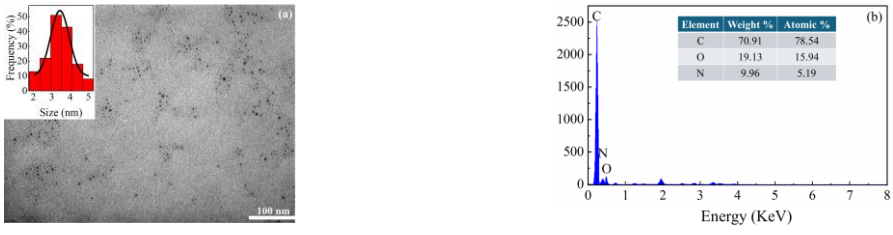

Figure 1. (a) TEM image (inset: particle size distribution of N-CQDs) and (b) EDS spectrum of N-CQDs

2.2.2. FTIR spectroscopy

FTIR spectroscopy was used to identify the surface functional groups of the synthesized N-CQDs. The results, presented in Figure 2, show that the N-CQDs exhibit surface groups such as O-H (hydroxyl) with a strong peak at 3329 cm^{-1} and N-H with a weak peak at 3287 cm^{-1}, which contribute to the good water solubility of the N-CQDs by forming hydrogen bonds with water molecules. The characteristic vibrations of C-H bonds were observed at 1047 cm^{-1} (C-H bending) and between 2892 and 2974 cm^{-1} (stretching modes of CH_2 and CH_3). Strong peaks corresponding to carbonyl C=O and carboxylic acid C=O groups were observed at 875 cm^{-1} and 1640 cm^{-1}, respectively, while a C-N stretching mode peak was noted at 1379 cm^{-1}. Furthermore, C-O stretching modes were observed at 1084 cm^{-1} [18]. These functional groups, characteristic of hydroxyl, carboxyl, and amino groups, along with N and O-containing molecules, and the absence of any impurity signals, confirm the successful functionalization of the N-CQDs and their high purity. FTIR analysis revealed the presence of C-N bonds, suggesting successful nitrogen incorporation into the carbon structure. However, the exact bonding configurations of nitrogen (pyridinic, pyrrolic, or graphitic nitrogen) and their specific contributions to the optical properties remain unclear without XPS analysis. Future work should focus on elucidating these details to further optimize the synthesis and properties of N-CQDs.

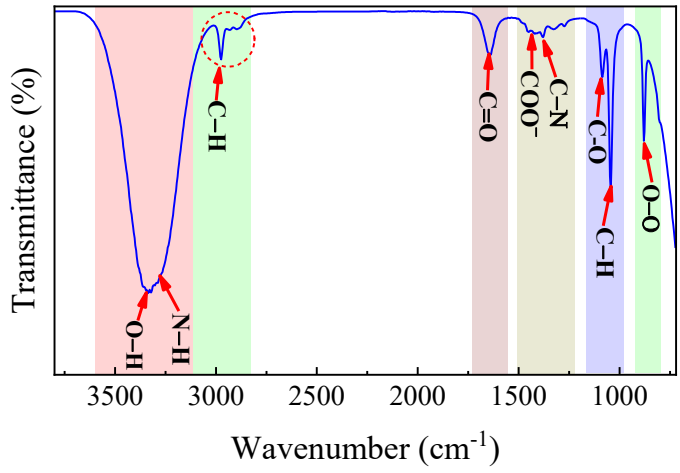

Figure 2. FTIR spectrum of N-CQDs

2.2.3. Optical properties of N-CQDs

The optical properties of the N-CQD sample are presented in Figure 3, showing the UV-Vis absorption spectrum, the photoluminescence (PL) spectrum, and the photoluminescence excitation (PLE) spectrum. The UV-Vis absorption spectrum (recorded in deionized water) of the N-CQDs exhibits a distinct peak at 262 nm, assignable to the π–π* transition of delocalized π electrons in the graphitic sp^2 domains within the sp^3 matrix, and a shoulder at around 355 nm, attributed to n–π* transitions of the C=O and C–N/C=N bonds [19].

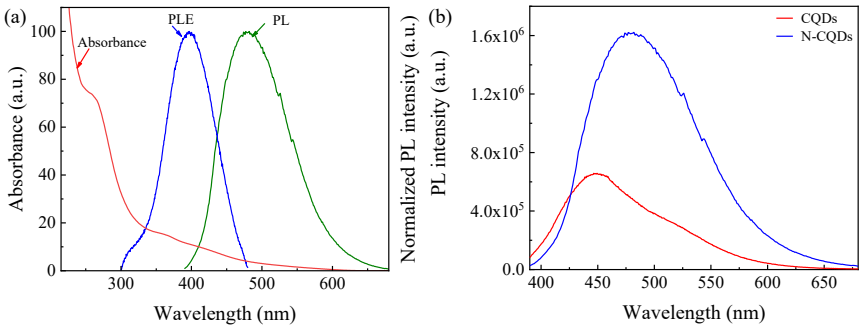

Figure 3. (a) UV-Vis absorption, excitation, and emission spectra of N-CQDs, (b) emission spectra of CQD and N-CQDs

The PLE spectrum shows a maximum excitation wavelength at 398 nm. When excited at this wavelength, the PL spectrum exhibits a maximum emission peak at 485 nm. For comparison, undoped CQDs synthesized under similar conditions showed a PL emission peak at 448 nm, while the N-CQDs exhibited a redshifted emission peak at 479 nm, accompanied by a significant increase in PL intensity (Fig. 3 (b)). This redshift and intensity improvement are attributed to the introduction of nitrogen-related energy levels, which modify the electronic structure and create additional radiative recombination pathways.

The synthesized N-CQDs exhibit a PLQY of 23%, which is a relatively high value compared to similar studies [20]. This strong fluorescence makes these N-CQDs promising candidates for various applications, such as in biosensors due to their high fluorescence, or in bioimaging, where their low toxicity and high quantum yield are beneficial. The enhanced fluorescence and quantum yield of N-CQDs compared to undoped CQDs can be attributed to the introduction of nitrogen atoms, which likely create additional surface states and improve electron-hole recombination efficiency. Previous studies have reported quantum yields (PLQYs) for N-CQDs synthesized from glucose and urea ranging from 9.6% to 81%, depending on the synthesis conditions, dopant ratios, and pH [21]. In this work, we achieved a PLQY of 23%, which is competitive and demonstrates the effectiveness of our simple, cost-effective hydrothermal synthesis method. While this value may not be groundbreaking, it highlights the potential of our approach for producing N-CQDs with good optical properties using environmentally benign precursors.

2.2.4. Effect of pH

The pH-dependent emission characteristics of the N-CQD samples were investigated by measuring the PL spectra of samples with pH values ranging from 2 to 9, using an excitation wavelength of 370 nm (Figure 4(a)). The trend in the PL peak intensity under different pH conditions is shown in Figure 4(b). Under pH conditions from 2 to 5, the PL intensity increases, reaching a maximum at pH 5. Subsequently, the intensity decreases as the pH increases from 6 to 9. The emission peak position remains almost unchanged across the pH range. The observed changes in PL intensity are likely due to protonation and deprotonation of surface functional groups such as carboxyl and

amino groups. At highly acidic pH (pH < 5), protonation of these groups results in the formation of neutral surface sites. This leads to N-CQD aggregation, ultimately decreasing the PL intensity due to increased fluorescence quenching. At pH 5, deprotonation of surface amino and carboxyl groups occurs, leading to the formation of a negatively charged shell that stabilizes the N-CQDs, resulting in an enhancement in fluorescence due to suppressed aggregation and increased electron-hole recombination. With increasing alkalinity (pH >5), excessive deprotonation creates an even stronger negatively charged surface shell on the N-CQDs, possibly leading to a decrease in emission intensity and the creation of electron trap states [22].

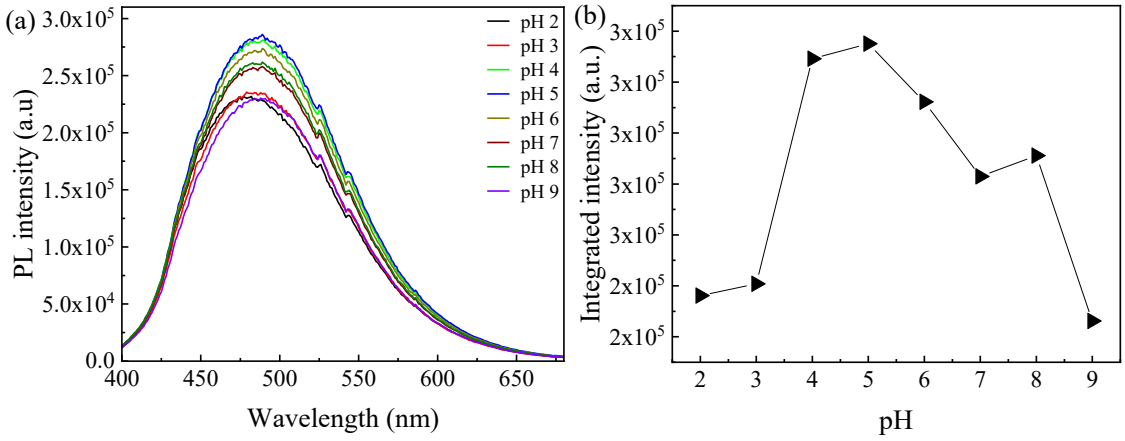

Figure 4. (a) Photoluminescence (PL) spectra and (b) the trend of integrated PL intensity of N-CQDs at different pH values

3. Conclusions

This study demonstrated a facile hydrothermal synthesis of N-CQDs using glucose and urea as environmentally friendly precursors. The synthesized N-CQDs exhibited an average size of 3.6 ± 0.57 nm, strong blue fluorescence at 485 nm, and a 23% quantum yield, enhanced by nitrogen doping. The pH-dependent fluorescence reached a maximum at pH 5.0, indicating tunable optical properties. These results suggest that N-CQDs are promising for bioimaging and sensing applications.

Acknowledgments. This research was funded by a research grant from the University of Medicine and Pharmacy, Hue University, with project code 42/24.

REFERENCES

[1] Wu L, Li Y, Liu GQ & Yu SH, (2024). Polytypic metal chalcogenide nanocrystals. *Chemical Society Reviews,* 53, 9832-9873.

[2] Nabil M & Megahed F, (2023). Quantum dot nanomaterials: preparation, characterization, advanced bio-imaging and therapeutic applications. *Journal of Fluorescence*, 34(6), 2467-2484.

[3] Barzegari S, Amani-Ghadim AR & Bayat F, (2024). Homogeneous embedding of plasmonic gold nanoparticles on FTO substrate to increase efficiency in CdS0.75Se0.25 quantum dot sensitized solar cell. *Solar Energy*, 277, 112656.

[4] Kim SH, Kim JY, Son DI & Lee HS, (2024). Heterointerface effects on carrier dynamics in colloidal quantum dots and their application to light-emitting diodes. *ACS Applied Materials and Interfaces*, 16(19), 25511-25518.

[5] Sobhanan J, Rival J V, Anas A & et al., (2023). Luminescent quantum dots: Synthesis, optical properties, bioimaging and toxicity. *Advanced Drug Delivery Reviews*, 197, 114830.

[6] Guan S & Tang M, (2024). Exposure of quantum dots in the nervous system: Central nervous system risks and the blood-brain barrier interface. *Journal of Applied Toxicology*, 44(7), 936-952.

[7] Yeh YJ, Liou JR, Lin W & et al., (2024). Plasma-engineered GQD-inorganic membranes with tunable interactions for ultrahigh-efficiency molecular separations. *Journal of Membrane Science*, 690, 122248.

[8] Syed N, Huang J & Feng Y, (2022). CQDs as emerging trends for prospect in enhancement of photocatalytic activity. *Carbon Letters*, 32(1), 81-97.

[9] Ahmed F, Zuhair Abbas Shah S, Ul Hassan N & et al., (2024). Band gap engineering of vacancy-ordered halide perovskite Cs2SnCl6 from substitutional doping of Pt (Cs2Sn(1-x)PtxCl6 where x = 0, 0.25, 0.50, 0.75 and 1.00) and its effects on thermoelectric properties using the first-principles approach. *Inorganic Chemistry Communications*, 164, 112461.

[10] Do TTH, Cao DN, Nguyen TH & et al., (2023). Control the solubility of carbon quantum dots by solvent engineering. *HPU2 Journal of Science: Natural Sciences and Technology*, 2(3), 51-58.

[11] Chipangura YE, Spindler BD, Bühlmann P & Stein A, (2024). Design criteria for nanostructured carbon materials as solid contacts for ion-selective sensors. *Advanced Materials*, 36(8), 2309778.

[12] Le TMO, Lam TH, Pham DC & Do DB, (2020). Synthesis and study of the physical and photocatalytic properties of composites g-C_3N_4ZnO. *Journal of Science Natural Science*, 65(3), 46-53.

[13] Tetteh IK, Issahaku I, Tetteh AY, (2024). Recent advances in synthesis, characterization, and environmental applications of activated carbons and other carbon derivatives. *Carbon Trends*, 14, 100328.

[14] Chaudhary N, Gupta PK, Eremin S, Solanki PR, (2020). One-step green approach to synthesize highly fluorescent carbon quantum dots from banana juice for selective detection of copper ions. *Journal of Environmental Chemical Engineering*, 8(3), 103720.

[15] Aup-Ngoen KK, Noipitak M, Sudchanham J & et al., (2024). The impact of carbon nanoparticles derived from sucrose, glucose, and fructose precursors on the performance of fully printed perovskite solar cells. *Materials Today Communications*, 39, 108549.

[16] Pho QH, Lin LL, Rebrov EV & et al., (2023). Process intensification for gram-scale synthesis of N-doped carbon quantum dots, immersing a microplasma jet in a gas-liquid reactor. *Chemical Engineering Journal*, 452, 139164.

[17] Dubey A & Dube CL, (2024). Microwave processing of carbon-based materials: A review. *Nano-Structures & Nano-Objects*, 38, 101136.

[18] MAA Joseph R, Kutti Rani S & Vasimalai N, (2024). A novel molecular imprinted polymer grafted on N, S Co-doped carbon quantum dots-based fluorescence sensor for chloramphenicol in food and clinical samples. *Microchemical Journal*, 207, 111675.

[19] Peng B, Xu J, Fan M & et al., (2020). Smartphone colorimetric determination of hydrogen peroxide in real samples based on B, N, and S co-doped carbon dots probe. *Analytical and Bioanalytical Chemistry*, 412(4), 861-870.

[20] Zhang L, Yang X, Yin Z & Sun L, (2022). A review on carbon quantum dots: Synthesis, photoluminescence mechanisms and applications. *Luminescence*, 37(10), 1612-1638.

[21] Shaik SA, Sengupta S, Varma RS & et al., (2021). Syntheses of N-Doped Carbon Quantum Dots (NCQDs) from Bioderived Precursors: A Timely Update. *ACS Sustainable Chemistry & Engineering*, 9(1), 3-49.

[22] Mokhine S, Aladesuyi OA, Masha S & Oluwafemi OS, (2024). Selective and sensitive determination of Folic acid amidst interfering metal ions and biomolecules using N-doped carbon quantum dots (N-CQDs). *Nano-Structures & Nano-Objects*, 37, 101085.